Astron. Astrophys. 346, 705–712 (1999)

ASTRONOMY AND ASTROPHYSICS

Experimental determination of the band oscillator strengths of the CO $A^1\Pi(11\leq v'\leq 23)$-$X^1\Sigma^+(v''=0)$ made at the LURE-SuperACO synchrotron facility.

M. Eidelsberg[1], **A. Jolly**[1], **J.L. Lemaire**[1,2], **W.-ÜL. Tchang-Brillet**[1,3], **J. Breton**[4,5], **and F. Rostas**[1]

[1] DAMAP et URA 812 du CNRS, Observatoire de Paris-Meudon, F-92195 Meudon Cedex, France
[2] Université de Cergy-Pontoise, Centre de Neuville, F-95031 Cergy-Pontoise Cedex, France
[3] Université Pierre et Marie Curie, 4 pl. Jussieu, F-75252 Paris Cedex 05, France
[4] Université Pierre et Marie Curie - ESVUV, Case 081, 4 pl. Jussieu, F-75252 Paris Cedex 05, France
[5] Université Paris-Sud, F-91405 Orsay Cedex, France

Received 10 August 1998 / Accepted 16 November 1998

Abstract. The band-integrated absorption oscillator strengths of the CO $A^1\Pi(11\leq v'\leq 23)$-$X^1\Sigma^+(v''=0)$ transition have been measured using monochromatized synchrotron radiation from the LURE-SuperACO facility as background source. The absorption spectra were analyzed using the simulation-fitting technique described in an earlier publication (Jolly et al. 1997). Up to v'=20, the results are in good agreement with very recent ab initio calculations (Spielfiedel et al. 1999) and VUV laser measurements(Stark et al. 1998). For v'=23 which is measured here for the first time, and for v'=21 the measured oscillator strengths are found to be significantly larger than the calculated ones. Combining experimental and calculated results, a set of recommended oscillator strengths is proposed.

Key words: molecular data – ISM: molecules – ultraviolet: ISM

1. Introduction

Being the second most abundant molecule in the interstellar medium, CO is widely used in place of H_2 which is not detectable as a tracer of molecular density. Mapping the intensity emitted by CO in the millimeter or infrared wavelength ranges allows a qualitative determination of the spatial distribution of molecular species over extended regions. Quantitative column densities, however, are obtained, for discrete lines of sight, by measuring the optical absorption of CO in the vacuum ultraviolet (VUV). Such measurements have become accessible with the advent of spectrographs observing from above the atmosphere on board the Copernicus, International Ultraviolet Explorer (IUE) and Hubble Space Telescope (HST), Far Ultraviolet Spectroscopic Explorer (FUSE) satellites (Morton & Noreau, 1994 and references therein, concerning FUSE see Sahnow et al. 1996). The precision of this technique is best when the lines or bands used for the measurement are not too saturated. In view of the wide range of column densities encountered, an equally wide range of absorption oscillator strengths is needed. In this respect the CO $A^1\Pi(v')$-$X^1\Sigma^+(v''=0)$ transition is extremely favourable since the band oscillator strengths vary over 6 orders of magnitude when v' varies between 0 and 23. This has been put to use for example in the determination of the relative abundances of various isotopic forms of CO by comparing the extinction of a set of strong and a set of weak bands of the rare and normal varieties respectively (Wannier et al. 1982; Sheffer et al. 1992; Lambert et al. 1994). The isotopic ratio deduced depends directly on the relative value of the oscillator strengths measured for the two sets of bands used.

The band oscillator strengths needed to determine absolute column densities have been measured by different techniques and calculated ab initio. Three experimental techniques have been used: electron energy loss (Chan et al. 1993; Zhong et al. 1997), band averaged lifetime measurements (Field et al. 1983) and optical absorption (Eidelsberg et al. 1992; Smith et al. 1994; Federman et al. 1997; Jolly et al. 1997; Stark et al. 1998). Ab initio calculations have been made by Kirby & Cooper (1989), Chantranoupong et al. (1992) and Spielfiedel et al. (1999, this issue, hereinafter AS). A thorough review of all the data available before 1997 can be found in the papers by Eidelsberg et al. (1992) and Chan et al. (1993). Only the most recent and/or the most comprehensive sets of data are considered below. Jolly et al. 1997 (hereinafter: AJ) discuss the merits and drawbacks of the various experimental techniques. The optical absorption technique appears as the most straightforward, provided the line saturation effects can be thoroughly taken into account in the data analysis. This effect was discussed at some length in AJ and by Malmasson et al. (1994). Briefly, it appears as a progressive decrease of the slope of the measured integrated and peak absorption vs. optical depth curves. This is due to the non linear nature of the convolution of the exponential absorption spectrum with the instrument function. The saturation increases as the ratio of the instrument to line width increases. The simplest way to eliminate the errors due to line saturation is to reduce the optical depth (i.e. the pressure) and to extrapolate to zero opti-

Send offprint requests to: M. Eidelsberg (eidelsberg@obspm.fr)

cal depth. When the instrumental width is large this may entail working at extremely low peak absorptions and the signal/noise ratio will set the low pressure limit and ultimately the precision of the absorption measurements. Jolly et al. (1997) showed that, by simulating the absorption spectra including the line saturation effect and least squares fitting the simulated spectra to the observed ones, it was possible to obtain reliable absorption cross sections even in the presence of strong line saturation effects. In that work the ratio of true to apparent band integrated cross sections was typically of 5 when the lines were not artificially pressure broadened. This strong line saturation effect was due to the fact that the benefit brought by the high spectral resolution of the VUV laser was partially offset by the relatively low signal/noise ratio which led to the use of higher peak absorptions.

Granted that the simulation-fitting technique can accommodate strong saturation situations, it opens the way to high quality measurements at low resolution provided the signal/noise ratio is high enough to measure very low peak absorptions. Thus it appears that, typical synchrotron radiation sources such as the LURE-SuperACO ring at Orsay, which delivers high photon fluxes with good stability at modest resolution, can be quite suited for such experiments. It is expected that the fitting technique will avoid the need for the sometimes risky extrapolation to zero pressure. Using a synchrotron radiation source opens the possibility of measuring A- X(v'-0) transitions up to the highest vibrational level of the A state (v'=23) while the tuning range of the VUV Laser in its present configuration limited the range covered in AJ to v'$\leq$17.

Studying the high lying vibrational levels of the CO $A^1\Pi$ state is important in several respects: i) The v'-0 bands absorb below 1200 Å for v'$\geq$16 making these bands potentially very useful to observe with the FUSE satellite ii) Their small oscillator strengths make them useful in the same context for probing high column density regions of molecular clouds provided the dust extinction is not too high. iii) The results provide an experimental verification of ab initio calculations of the electronic transition moment over a wider range of internuclear distances where significant discrepancies exist. These distances gain in importance for transitions involving higher vibrational levels of the ground state. Such transitions may be observed in absorption when the gas temperature increases and in emission in plasmas. iv) Often neglected effects have to be taken into account in the quantitative analysis of the line and band intensities, namely: the breakdown of the r-centroid approximation above v'$\approx$12 and the vibration-rotation interaction for v' above $\approx$17 and J above $\approx$20.

The experimental part of the present work was conducted on the LURE SuperACO synchrotron ring using monochromatized light with a spectral line width of 0.5 to 1.0 Å. The band integrated absorption cross sections of the A-X (v'-0) transitions were measured for 11$\leq$v'$\leq$23. No published results were available for v'$>$17 when these measurements were undertaken. In the meantime the results of G.Stark et al.(1998) concerning v'=13,14,16,18,19,20 and 21 were communicated to us prior to publication. The general conclusion of the present study is that up to v'=20 these two recent sets of measurements are in good agreement with one another and with the new ab initio calculations of AS. It is found that, considering the amount of converging information now available, it is reasonable at this point to propose a new set of recommended oscillator strengths for the $A^1\Pi(v')$-$X^1\Sigma^+(v''=0)$ bands replacing those of Morton & Noreau (1994).

2. Experiments

2.1. Experimental setup

The experiments were conducted on the SuperACO synchrotron ring at Orsay using the SA61 beam line. This line is equiped with a 3 metre, f/30 normal incidence concave grating monochromator. A 1200 lines/mm grating was used with 200 μm slits. The light emerging from the 3 metre monochromator traversed a 48 cm long, 100 mm diameter stainless steel cell closed on one end by a MgF_2 window and on the other by a fused silica window coated on the inner side with a thin layer of sodium salicylate. The visible light emitted by the coating when illuminated by the VUV light fell on a 50mm diameter S20 (multialkali) photocathode photomultiplier tube (PMT) placed immediately after the output window. The cell was pumped by a 100 l/s turbomolecular pump. After outgassing, the base pressure was below 10^{-6} Torr and CO gas (Air Liquide 99.995 purity) was introduced in the cell from a 100 atm tank fitted with a pressure controller. Filling pressures ranging from 10^{-2} to 200 Torr were measured with one of a pair of capacitance manometer heads of 10 and 1000 Torr full scale sensitivity respectively (Datametrics Barocell 590Q series, accuracy: $5x10^{-5}$ of full scale).

The data were recorded on a PC using a home made software which drove the grating and recorded the signal from the photomultiplier. The DC current from the anode was converted by a Keithley type 427 electrometer amplifier into a voltage which was read by a 12 bit analog to digital conversion card (EUROSmart Fr. Fastlab). The dynamic range was increased by recording simultaneously the data in three channels with different gains. The PMT output corresponding to the unabsorbed background flux was typically of 10^{-6} A. The time constant of the current amplifier was set at 1 msec. The data acquisition rate was generally set at 3 samples/sec and the wavelength scanning speed at 0.15 Å/s. The slit widths of the monochromator were generally set at 200 μm. The instrument width was measured using the Xe line at 1192.5 Å as a standard and found to be of 0.70 Å. This value is consistently confirmed when it is left free in the spectrum fitting procedure described below. The wavelength steps, scanning speed and data averaging windows are optimized in order to insure that the instrument width is not degraded.

Typical spectra are displayed on Fig. 4. It is seen that absorptions of 2% can be routinely measured. The peak to peak noise of the traces is typically of 0.5%. This is larger than the expected photon noise which should be in the range of 0.01% for a measured count rate of the order of 10^6 s^{-1}. The trace noise is probably due mostly to the beam instability compounded by residual vibrations of the experimental platform.

2.2. Data analysis

The determination of line oscillator strengths from absorption spectra is based on the Beer- Lambert law

$$I(\lambda) = I_0(\lambda)e^{-\tau(\lambda)}$$

where I and I_0 are the transmitted and incident intensities respectively and $\tau(\lambda)$ is the optical depth profile of the feature (line or band):

$$\tau(\lambda) = nl\sigma(\lambda) = N\sigma_T F(\lambda) = 8.85 \times 10^{-21}\lambda^2 N f F(\lambda)$$

where: n is the volume density of the absorbing particles in the medium (in $cm^{-3)}$, l its length (in cm) and N=n l its column density (in cm^{-2}). $\sigma(\lambda)$ and σ_T are respectively the absorption cross section profile and the line integrated absorption cross section (in cm^2 and cm^2 Å respectively). $F(\lambda)$ is the normalized profile ($\int F(\lambda)d\lambda = 1$) and f is the oscillator strength of the feature, λ is the wavelength in Å.

Experimentally, in the ideal case where the instrumental resolution is infinite, $\tau(\lambda)$ is obtained directly from the transmitted intensity:

$$\tau(\lambda) = log_e(I_0(\lambda)/I(\lambda))$$

and the integrated cross section and oscillator strength are deduced from the area under the profile $\tau(\lambda)$ of the feature:

$$\int \tau(\lambda)d\lambda = N\sigma_T \int F(\lambda)d\lambda = N\sigma_T = 8.85 \times 10^{-21}\lambda^2 N f$$

However, as discussed in AJ, the applicability of this procedure is limited by the line saturation effect that results from the fact that the measured spectrum is the convolution of the intrinsic absorption spectrum by an instrumental profile $P(\lambda)$

$$\begin{aligned} I(\lambda)_{meas} &= \int P(\lambda - \lambda')I(\lambda')d\lambda' \\ &= \int P(\lambda - \lambda')I_0(\lambda')e^{-\tau(\lambda')}d\lambda' \end{aligned}$$

If $I_0(\lambda)$ is a slowly varying function

$$I(\lambda)_{meas} \approx I_0(\lambda) \int P(\lambda - \lambda')e^{-\tau(\lambda')}d\lambda' \qquad (1)$$

It is seen that, in this expression, the absorption spectrum $\tau(\lambda)$ is the argument of an exponential. This expression is different from the standard ("linear") convolution that applies when an emission spectrum is recorded with a finite instrument width. While the standard convolution conserves the area of the spectral features, the "non-linear" convolution involving an exponential of the profile, that applies in absorption, does not. This amounts to a saturation effect that causes both the peak absorption and the area of the features recovered through the expression

$$\tau(\lambda)_{meas} = log_e(I_0/I)$$

to be reduced from those of the intrinsic absorption profile. The saturation effect increases with τ and with the ratio (R) of the instrumental to line widths. This effect obviously affects also

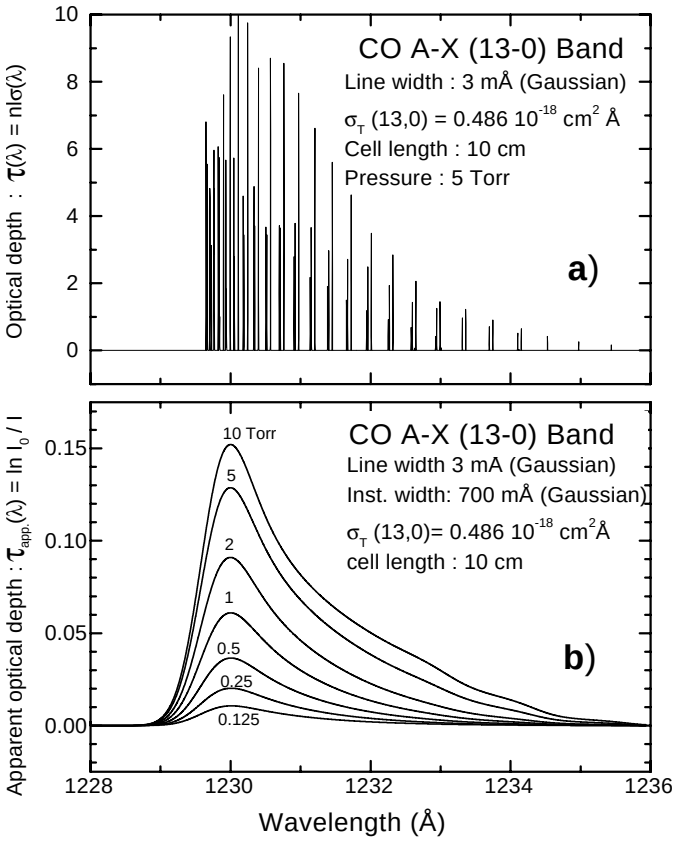

Fig. 1a and b. Simulated absorption spectra of the A-X (13-0) band **a** Intrinsic absorption spectrum. **b** Convolution of the intrinsic band absorption spectrum with the instrument profile.

the band integrated absorption cross sections, which are defined as:

$$\sigma_{v',v''} = \sigma_T(v', v'') = \Sigma_{band}\sigma_T(v'J', v''J'') = \int_{band} \sigma(\lambda)d\lambda$$

The line saturation effect is illustrated in Figs. 1 and 2 where the 13-0 band has been simulated, as described below, for experimental conditions illustrative of the present set of data i.e. pressure-length product: p.l≤100 Torr.cm and, instrument width: $\Delta\lambda = 700m$Å. It is seen that the apparent (i.e. measurable) parameters are very strongly reduced from the true ones even for very small optical depths. It is worth mentionning that the error thus introduced on the band integrated cross section depends on the details of the rotational structure (i.e. intensity distribution in the band, line overlaps...) and not only on the instrument to line width ratio. Therefore it is not possible to build a curve of growth that could be used for all the bands, so that each band has to be treated separately.

In most optical absorption experiments the line saturation effect is treated by an extrapolation to zero pressure of the measured cross sections. This procedure is applicable as long as R is not too high. Otherwise it becomes necessary to record the spectra at such low optical depths that the signal/noise ratio becomes too low and the precision of the measurements becomes insufficient. It is seen on Fig. 2a that, for an instrumental line

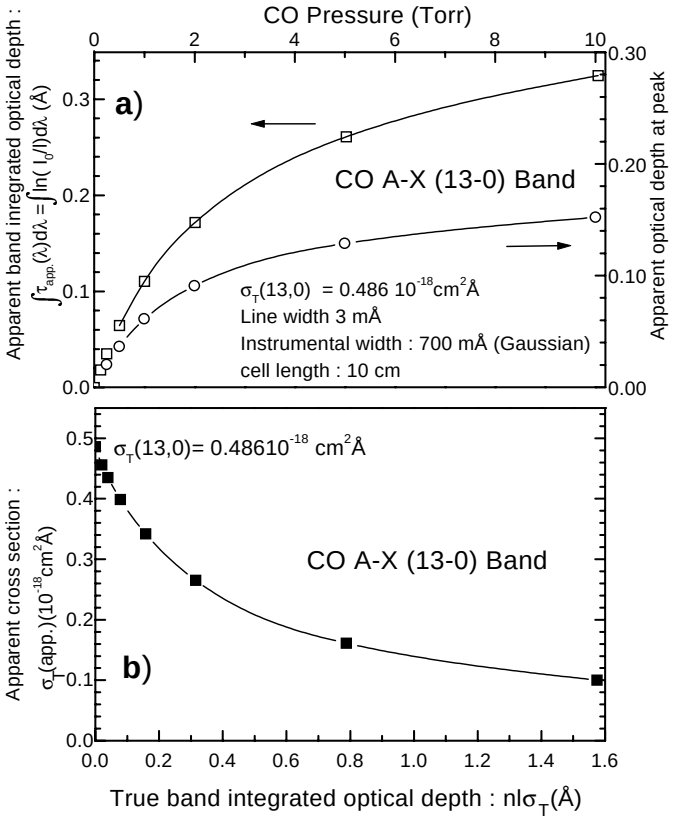

Fig. 2a and b. Simulation of the instrumental saturation effects on the A-X (13-0) band **a** Apparent vs. true band integrated optical depth. **b** Variation of the apparent band integrated cross section with true optical depth.

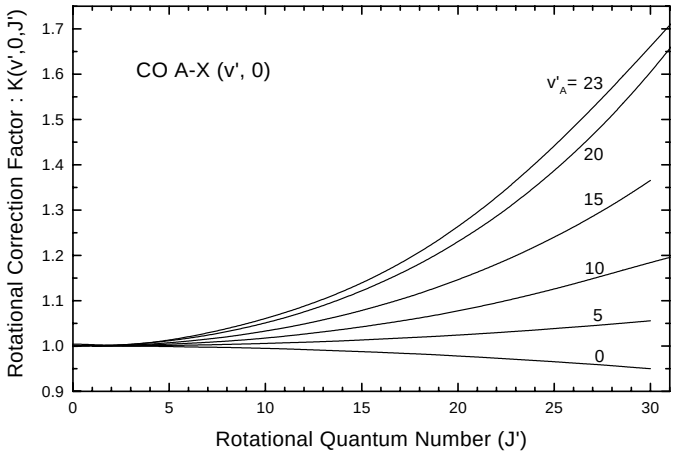

Fig. 3. Centrifugal distortion correction factor

width of 700 mÅ, i.e. a line width ratio R=233 it is necessary to reduce the peak optical depth of the band below 1% in order to allow a safe linear extrapolation to zero absorption. The signal/noise ratio of our present experiments would marginally allow such a procedure. However we have found it much more expedient to use the simulation-fitting technique that was set up for the CO A-X bands in AJ. This method allows the use of much stronger absorptions and thus considerably improves the accuracy of the measured cross sections.

The details of the method have been described in AJ (Jolly et al. 1997). Briefly, the optically thin absorption spectrum of each band is calculated using the spectroscopic data of Simmons et al. (1969), R.W.Field (1971, 1972) and A. Le Floch (1987, 1989) which provide, for each line of a band, its position and the change in its intensity caused by perturbations in terms of its fractional Π-character (C^2). The line intensities are calculated using the standard intensity factors for $A^1\Pi - ^1\Sigma$ transition multiplied by the proper C^2 factor when needed. For high lying vibrational levels the vibration-rotation interaction has to be introduced for high rotational quantum numbers. This interaction comes from the centrifugal distortion which appears when the rotational energy is added to the rotationless potential curves (see below). The correction factors $K^2(v', v'', J')$ to be applied for the A-X (v'-0) bands are plotted on Fig. 3. It is seen that at J=20 the correction exceeds 10% for v'>17. However the weight of the high J lines in the band integrated cross sections is relatively low so that the correction exceeds 5% above v'=19 only and reaches 7% for v'=23. If the measurement relies heavily on high J lines, as in the work of Stark et al. (1998), the correction has to be evaluated in every case.

Taking into account the normalized rotational population distribution $n_N(J'', v'', T) = n(J'', v'', T)/n(v'', T)$ corresponding to the proper temperature, the line integrated cross sections can be written as:

$$\begin{aligned}&\tau_T(v'J', v''J'')\\ &\quad = l.n(v'', T)\sigma(v', v'')\\ &\qquad \times\{n_N(J'', v'', T)K^2(v', v'', J'')C^2(v', J')\mathbf{S}(\mathrm{J}', \mathrm{J}0'')\}\end{aligned} \tag{2}$$

where $\sigma(v', v'')$ is the band integrated cross section calculated from the rotationless potential curves, $K^2(v', v'', J'')$ is the centrifugal distortion correction term, C^2 is the fractional Π-character of the upper level of the perturbed line and **S** (J',J") is the rotational line strength with

$$S(\mathrm{J}', \mathrm{J}'') = \mathcal{S}(\mathrm{J}', \mathrm{J}'')/2(2\mathrm{J}'' + 1)$$

for $A^1\Pi - ^1\Sigma$ transition. The Hönl-London factors $\mathcal{S}(\mathrm{J}', \mathrm{J}'')$ are equal to J"-1, 2J"+1 and J"+2 respectively for P, Q and R branches, so that $\Sigma_{J'}\mathbf{S}(\mathrm{J}', \mathrm{J}'') = 1$ for unperturbed lines and $\Sigma_{J'}\alpha^2(v', J')\mathbf{S}(\mathrm{J}', \mathrm{J}'') = 1$ for perturbed lines (i.e. main + extra lines). The term in curly brackets thus represents the normalized band spectrum, i.e. such that the sum of the line intensities equals unity. It is placed on an absolute optical depth scale by multiplying it successively by the path length, l, the absorber density in the lower vibrational state of the transition, n(v",T), at the temperature of the experiment, and the rotationless band integrated cross section $\sigma(v', v'')$.

The optically thin spectrum of a (v',v") band is then obtained by adding at each wavelength the contribution of all the individual lines included in the band:

$$\tau(\lambda) = \Sigma_{band}\tau_T(v'J', v''J'')F(\lambda - \lambda_{v'J', v''J''})$$

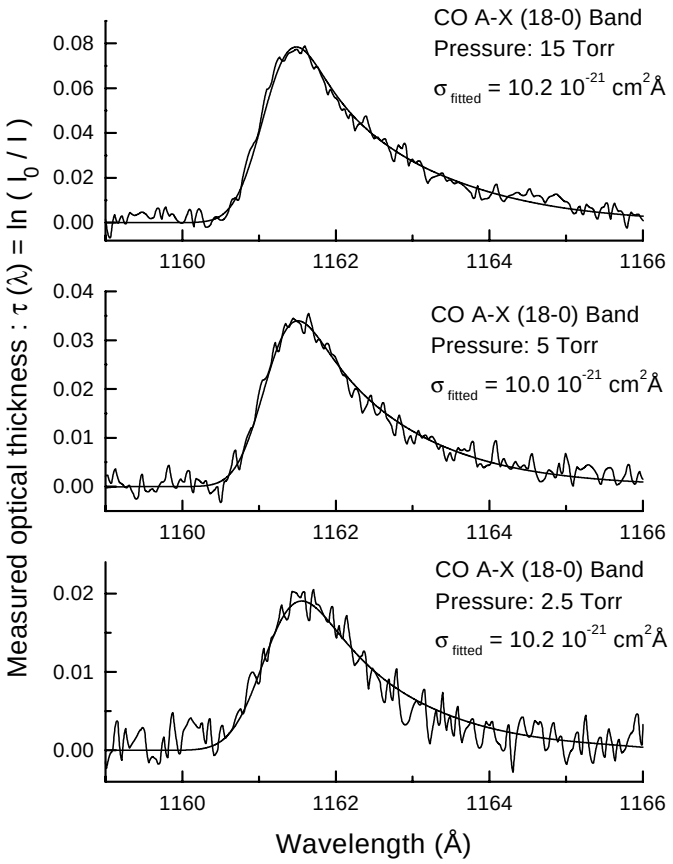

Fig. 4. Experimental and fitted absorption spectra of the 18-0 band at various pressures

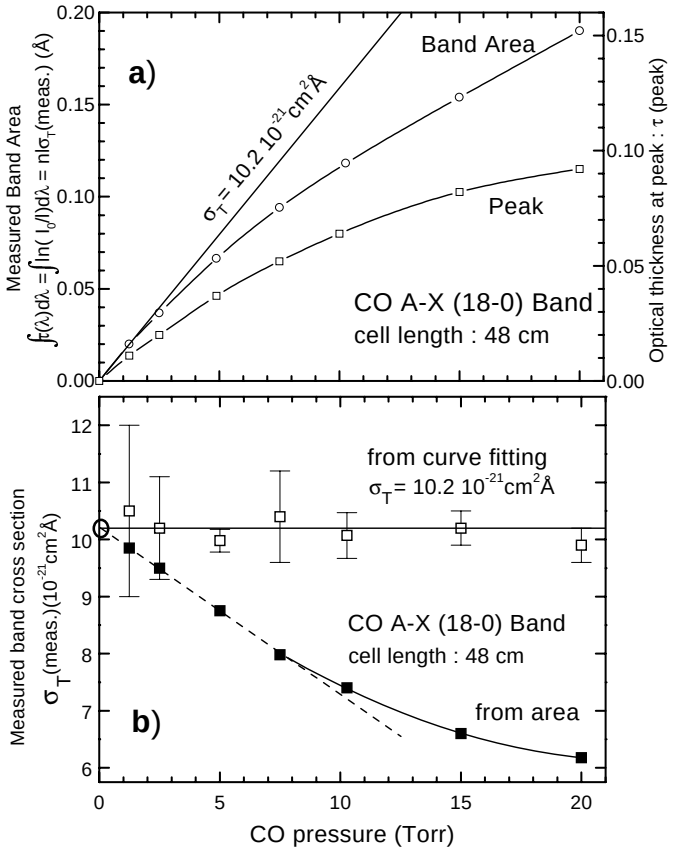

Fig. 5a and b. Pressure dependence of the 18-0 band measurements. **a** Band area and peak absorption **b** Cross sections measured through the subtended area and by the simulation/fitting technique

where $F(\lambda)$ is the intrinsic line profile. In the present case, the CO pressure is kept low enough to ensure that collisional broadening is negligible and the lines have a Doppler profile with a width determined by the experimental temperature.

The optically thin spectrum is then convolved with the instrument profile $P(\lambda)$ according to Eq. (1) in order to obtain the calculated spectrum $\tau(\lambda)_{calc}$. The instrument profile is taken as Gaussian with a width determined largely but not entirely by the slit widths of the monochromator. The calculated spectrum is least squares fitted to the measured spectrum:

$$\tau(\lambda)_{meas} = log_e I_0(\lambda)/I(\lambda)$$

with the band integrated cross section $\sigma(v', v'')$ and the instrumental width being left free in the fitting procedure.

A typical set of experimental and fitted spectra obtained in a range of CO pressures is displayed on Fig. 4. Fig. 5a illustrates the non linear behaviour of the band-integrated and peak absorptions. It is seen on Fig. 5b that, over this range of pressures, the apparent cross section, as deduced from the area subtended by the band, decreases with increasing pressure while the fitted cross section stays constant. When the pressure is low enough, the apparent cross section tends towards the fitted one and a linear extrapolation to zero pressure gives a result in agreement with the result obtained by fitting.

3. Results and discussion

3.1. CO A-X bands

The (v'-0) band absorption cross sections have been measured for $11\leq v'\leq 23$ at pressures varying from 0.02 to 200 Torr with a cell length of 48 cm. The v'=19 and 22 bands could not be measured because they are burried under the $B^1\Sigma^+ - X^1\Pi$ (0-0) and (1-0) bands. The v'=20 and 23 bands appear as weak features on the far blue wings of the same bands while v'=21 is on the red wing of the B-X(1-0) band. For each band the CO pressure was varied over a range allowing the peak absorption to vary from 1 or 2% to about 10%. The band integrated cross section was determined both by the simulation/fitting technique and by measuring the area under the band. In order to calculate the optical depth $\ln(I_0/I)$, the baseline I_0 was determined by fitting a smooth curve bridging the baseline across the absorption band. Diagrams similar to that of Fig. 5b were obtained in each case, ensuring that line saturation effects were properly taken care of. The results obtained are summarized in Table 1 where the oscillator strengths are calculated from the cross sections through the formula

$$f_{v'v''} = 1.13 \times 10^{20} \lambda^{-2} \sigma_{v'v''}$$

(where λ is in Å and $\sigma_{v'v''}$ in cm^2 Å). They are compared to other pertinent experimental and theoretical results in Table 2

Table 1. Experimental results. Numbers in parentheses are the powers of 10 multiplying the results listed. The Franck-Condon factors used to calculate f/q are listed in Table 2

v'	(v'-0) Bandhead λ (Å)	CO Pressure (Torr)	Cross section $\sigma_{v',0}$ (cm^2.Å)	Oscillator strength $f_{v',0}$	Reduced Oscillator strength $f_{v',0}/q_{v',0}$
11	1263	0.02-0.1	2.92 ± 0.29 (-18)	2.07 ± 0.20 (-4)	0.382 ± 0.04
12	1246	0.04-0.2	1.26 ± 0.13 (-18)	9.17 ± 0.10 (-5)	0.409 ± 0.04
13	1230	0.1-0.7	4.86 ± 0.49 (-19)	3.63 ± 0.36 (-5)	0.393 ± 0.04
14	1214	0.12-1	2.35 ± 0.23 (-19)	1.80 ± 0.18 (-5)	0.476 ± 0.05
15	1200	0.2-2	1.07 ± 0.11 (-19)	8.40 ± 0.84 (-6)	0.542 ± 0.05
16	1186	0.5-3	4.67 ± 0.47 (-20)	3.75 ± 0.38 (-6)	0.587 ± 0.06
17	1173	1-15	2.02 ± 0.20 (-20)	1.66 ± 0.17 (-6)	0.625 ± 0.06
18	1161	1.25-30	1.02 ± 0.10 (-20)	8.54 ± 0.85 (-7)	0.763 ± 0.07
19	1150	–	–	–	–
20	1140	15-55	2.20 ± 0.22 (-21)	1.93 ± 0.19 (-7)	0.919 ± 0.09
21	1130	30-100	1.20 ± 0.12 (-21)	1.06 ± 0.11 (-7)	1.123 ± 0.15
22	1122	–	–	–	–
23	1115	60-200	4.50 ± 0.90 (-22)	$4{,}00 \pm 0.80$ (-8)	1.970 ± 0.40

Table 2. Comparison of experimental and theoretical band oscillator strengths

	Experiment							Theory			Recommended values	
v'	This work (1998)	Stark et al. (1997)	Jolly et al. (1997)	Zhong et al. (1997)	Feder--man et al. (1997)	Smith et al. (1994)	Chan et al. (1993)	Spiel--fiedel et al. (1998)	Kirby & Cooper (1989)	q(v´ , 0) Spielfiedel et al. (1998)	Morton & Noreau (1994)	Present
0				1.66(-2)			1.62(-2)	1.50(-2)	1.55(-2)	1.217(-1)	1.62(-2)	1.66(-2)
1				3.38(-2)			3.51(-2)	3.13(-2)	3.23(-2)	2.276(-1)	3.51(-2)	3.45(-2)
2							4.02(-2)	3.59(-2)	3.72(-2)	2.355(-1)	4.02(-2)	3.95(-2)
3				3.25(-2)			3.47(-2)	3.02(-2)	3.15(-2)	1.796(-1)	3.47(-2)	3.33(-2)
4				2.23(-2)			2.42(-2)	2.09(-2)	2.20(-2)	1.134(-1)	2.42(-2)	2.30(-2)
5				1.41(-2)			1.45(-2)	1.27(-2)	1.34(-2)	6.295(-1)	1.45(-2)	1.40(-2)
6				7.7(-3)			8.05(-3)	7.03(-3)	7.48(-3)	3.195(-2)	8.05(-2)	7.76(-3)
7				4.3(-3)	3.5(-3)		4.14(-3)	3.64(-3)	3.90(-3)	1.519(-2)	4.14(-3)	4.02(-3)
8				2.3(-3)	1.69(-3)		2.02(-3)	1.80(-3)	1.93(-3)	6.892(-3)	2.02(-3)	1.98(-3)
9			9.61(-4)		7.8(-4)		9.5(-4)	8.54(-4)	9.24(-4)	3.020(-3)	9.50(-4)	9.42(-4)
10			4.16(-4)		3.5(-4)		4.1(-4)	3.96(-4)	4.30(-4)	1.290(-3)	4.10(-4)	4.36(-4)
11	2.07(-4)		2.02(-4)		1.3(-4)	1.7(-4)	1.8(-4)	1.80(-4)	1.96(-4)	5.416(-4)	1.80(-4)	1.99(-4)
12	9.17(-5)		—			6.9(-5)	9.0(-5)	8.10(-5)	8.83(-5)	2.245(-4)	9.00(-5)	8.93(-5)
13	3.63(-5)	4.04(-5)	3.62(-5)			3.7(-5)		3.63(-5)	3.94(-5)	9.232(-5)	3.47(-5)	4.00(-5)
14	1.80(-5)	1.87(-5)	1.66(-5)			1.5(-5)		1.63(-5)	1.75(-5)	3.783(-5)	1.44(-5)	1.80(-5)
15	8.40(-6)	—	7.14(-6)					7.37(-6)	7.74(-6)	1.551(-5)	5.94(-6)	8.12(-6)
16	3.75(-6)	3.86(-6)	3.13(-6)					3.37(-6)	3.43(-6)	6.390(-6)	2.46(-6)	3.72(-6)
17	1.66(-6)	—	1.31(-6)					1.56(-6)	1.52(-6)	2.656(-6)	1.02(-6)	1.72(-6)
18	8.54(-7)	8.50(-7)						7.37(-7)	6.77(-7)	1.119(-6)	4.30(-7)	8.12(-7)
19	—	—						3.53(-7)	3.02(-7)	4.795(-7)	1.83(-7)	3.89(-7)
20	1.93(-7)	1.87(-7)						1.72(-7)	1.35(-7)	2.101(-7)	8.01(-8)	1.90(-7)
21	1.06(-7)	9.90(-8)						8.60(-8)	6.07(-8)	9.436(-8)	3.58(-8)	1.02(-7)
22	—	—						4.42(-8)	2.72(-8)	4.346(-8)	1.63(-8)	5.64(-8)
23	4.00(-8)							2.31(-8)	1.21(-8)	2.031(-8)	7.88(-9)	3.16(-8)

where only the more recent data sets have been listed. A more complete comparison is available in AJ for $v' \leq 17$.

The theoretical results listed have been obtained from the ab initio transition moments using the proper vibrational averaging and not the r-centroid approximation which breaks down above v'≤12. Thus:

$$f_{v'v''} = 3.038 \times 10^{-6} \nu_{v'v''} g (D_{v'v''})^2$$

where:

$$D_{v'v''} = \langle \Psi(v') | R_e(r) | \Psi(v'') \rangle$$

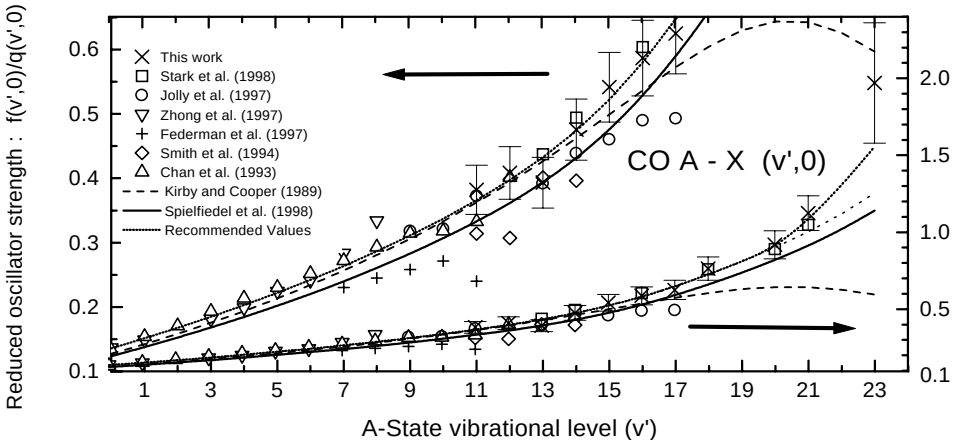

Fig. 6. Comparison of experimental and theoretical results. For clarity, the results for $0\leq v'\leq 17$ have been replotted on an expanded scale. Up to v'=20, the recommended values are obtained by multiplying the *ab initio* results of Spielfiedel at al. (1999) by 1.1. For v'=23, the recommended value is the average of the experimental and theoretical results.

is the rotationless vibrationally averaged dipole transition moment, $R_e(r)$ is the electronic transition moment and g is the statistical weight (g=2 for a $\Pi \leftarrow \Sigma$ transition). Strictly speaking, one should consider rotationally dependent line oscillator strengths f(v'J',v"J") calculated from

$$D(v'j', v''J'') = \langle \Psi(v'J')|R_e(r)|\Psi(v''J'')\rangle$$

However, it is convenient, to express the line oscillator strength as the product of a rotationless vibrational term and a rotational term (Larsson 1983). This is perfectly justified as long as the centrifugal distortion can be neglected. If such is not the case, this effect can be introduced as a correction:

$$D(v'J', v''J'') = D(v', v'')K(v'J', v''J'')$$

with

$$K(v'J', v''J'') = \langle \Psi(v'J')|R_e(r)|\Psi(v''J'')\rangle / \langle \Psi(v', 0)|R_e(r)|\Psi(v'', 0)\rangle$$

Since we are concerned here with a correction term only, it is justified to calculate it in the r-centroid approximation and for Q-branch lines only (J'=J"), which yields:

$$K(v'J', v''J') = \langle \Psi(v'J')|\Psi(v''J')\rangle / \langle \Psi(v', 0)|\Psi(v'', 0)\rangle$$

and the correction term introduced in Eq. (2) reads

$$[K(v', v'', J')]^2 = q(v'J', v''J'')/q(v', v'')$$

The *ab initio* calculations available are those of Kirby & Cooper (1989) and the new ones obtained by AS. The rotationless Franck-Condon factors listed in Table 2 have been obtained from the RKR potential curves of the $A^1\Pi$ and $X^1\Sigma^+$ states as discussed in AS.

The reduced oscillator strengths $(f_{v',0}/q_{v',0})$, introduced in AJ in order to compensate the effect of the strong variation of the vibrational overlap integrals for the wide range values of v'-v" values considered, are plotted in Fig. 6 from the data of Table 2. This plot reveals a very clear trend that stems from the agreement of several measurements and theoretical evaluations for each vibrational level up to v'=20. Below v'=15 the experimental results seem in better agreement with the ab initio calculations of Kirby and Cooper (1989). The converse is true between v'=16 and 20. For v'=21 both experimental values are significantly above the AS calculations. For v'=23, only the present experimental value is available. It is 50% above the theoretical value of AS et al. but the general trend is respected. We feel that this disagreement could be at least partially due to residual problems connected to the vibrational averaging of the transition moment and more specifically to uncertainties in the determination of the RKR potential near the dissociation limit. and, for the time being, the average between the two values seems a reasonable guess.

As suggested by Gibson (1998), the available data is well represented, up to v'=20, by the results of AS after the latter have been arbitrarily multiplied by a factor 1.1. This correction produces a very close fit as can be seen on Fig. 6. It is also seen that v'=21 and 23 deviate from this curve. It is proposed here to adopt, as a set of recommended oscillator strengths, 1.1 times the AS values up to v'=20, the average of the experimental values for v'=21 and the average of the present experiment and ab initio values for v'=23. These recommended values are listed in Table 2 and plotted as f/q on Fig. 6.

4. Conclusions

The present set of oscillator strength measurements for the $A^1\Pi(11 \leq v' \leq 23) - X^1\Sigma^+(v'' = 0)$ transition, combined with the new ab initio calculations of Spielfiedel et al. (1999, this issue) and earlier experimental data lead to a hopefully definitive set of recommended oscillator strengths at least for the range $0 \leq v' \leq 20$. In this range the majority of the experimental and calculated values agree within 10% error bars. For v'= 21 and 23 the experimental values are significantly larger than the calculated ones. This discrepancy is tentatively attributed to minor imperfections in the A-state RKR potential which is used in the calculations and which, for v'=23, is slightly above the dissociation limit and hence difficult to determine.

Acknowledgements. This work was supported in part by CNRS through the Programme National de Physique et Chimie de la Matière Interstellaire (PCMI). The authors acknowledge the support of LURE

through beam-time allocation. Thanks are also due to G. Stark for communicating experimental results prior to publication.

References

Chan W.F., Cooper G., Brion C.E., 1993, Chem. Phys. 170, 123
Chantranupong L., Bhanuprakash K., Honigmann M., Hirsch G., Buenker R.J., 1992, Chem. Phys. 161, 351
Eidelsberg M., Rostas F., Breton J., Thieblemont B., 1992, J. Chem. Phys. 96, 5585
Federman S.R., Menningen K.L., Lee Wei, Stoll J.B., 1997, ApJ 477, L61
Field R.W., 1971, Thesis Harvard University
Field R.W., Wicke B.G., Simmons J.D., Tilford S.G., 1972, J. Molec. Spectrosc. 44, 383
Field R.W., Benoist d'Azy O., Lavolée M., Lopez-Delgado R., Tramer A., 1983, J. Chem. Phys. 78, 2838
Gibson S.T., 1998, Private communication
Jolly A., Lemaire J.L., Belle-Oudry D., et al., 1997, J. Phys. B: At. Mol. Opt. Phys. 30, 4315
Kirby K., Cooper D.L., 1989, J. Chem. Phys. 90, 4895
Lambert D.L., Sheffer Y., Gilliland R.L., Federman S.R., 1994, ApJ 420, 756
Larsson M., 1983, A&A 128, 291
Le Floch A., 1989, Thesis, Université de Paris-Sud
Le Floch A., 1991, Molec. Phys. 72, 133
Le Floch A., Launay F., Rostas J., et al., 1987, J. Molec. Spectr. 121, 337
Malmasson D., Vient A., Lemaire J.L., et al., 1994, In: Nenner I. (ed.) AIP Conf. Proc. 312, AIP Press, New York, p. 349
Morton D.C., Noreau L., 1994, ApJS 95, 301
Sahnow D.J., et al., 1996, Proc. SPIE 2807, 2
Sheffer Y., Federman S.R., Lambert D.L., Cardelli J.A., 1992, ApJ 397, 482
Simmons J.D., Bass A.M., Tilford S.G., 1969, ApJ 155, 345
Smith P.L., Stark G., Yoshino K., Ito K., 1994, ApJ 431, L413
Spielfiedel A., Tchang-Brillet W.-Ü.L., Dayou F., Feautrier N., 1999, A&A (this issue)
Stark G., Lewis B.R., Gibson S.T., England J.P., 1998, ApJ 505, 453
Wannier P.G., Penzias A.A., Jenkins E.B., 1982, ApJ 254, 100
Zhong Z.P., Feng R.F., Xu K.Z., et al., 1997, Phys. Rev. A. 55, 1997